Moreno-Boza, D.; Iglesias, I.; Sánchez, A.L. Large-activation-energy analysis of gaseous reacting flow in pipes. In: *Combustion and flame, Vol. 178, April 2017, Pp. 217-224*

DOI: https://doi.org/10.1016/j.combustflame.2017.01.010

Large-activation-energy analysis of gaseous reacting flow in pipes

Daniel Moreno[a], Immaculada Iglesias[b], Antonio L. Sánchez[a]

[a] *Dept. Mechanical and Aerospace Engineering, University of California San Diego, La Jolla CA 92093-0411, USA*

[b] *Grupo de Mecánica de Fluidos, Universidad Carlos III de Madrid, Leganés 28911, Spain*

Abstract

This paper analyzes the exothermic reaction of an initially cold gaseous mixture flowing with a moderately large Reynolds number along a cylindrical pipe with constant wall temperature. An overall irreversible reaction with an Arrhenius rate having a large activation energy is used for the chemistry description. The flow is chemically frozen in the cold entrance region, where the velocity evolves towards the Poiseuille profile as the gas temperature increases towards the wall value, ushering in a reaction stage during which the rate of heat transfer from the wall changes from positive to negative. The subsequent downstream evolution of the flow depends critically on the competition between the heat released by the chemical reaction and the heat-conduction losses to the wall, as measured by the Damköhler number δ, first introduced by Frank-Kamenetskii in his seminal analysis of thermal explosions in cylindrical vessels. For values of δ below the critical value $\delta = 2$ corresponding to the quasi-steady explosion limit, heat losses to the wall keep the gas temperature close to the wall value, so that the chemical reaction occurs slowly along the pipe in a flameless mode, which is analyzed to give an implicit expression for the streamwise reactant distribution. By way of contrast, for $\delta > 2$ the slow reaction rates occur only in an initial ignition region, which ends abruptly when very large reaction rates cause a temperature runaway, or thermal explosion, at a well-defined location, whose computation must account for the temperature found at the end of the entrance region. The predictions of the large-activation energy analyses, including ignition distances for $\delta > 2$ and flameless reactant consumption rates for $\delta < 2$, show good agreement with numerical computations of the reactive pipe flow for finite values of the activation energy.

Keywords: activation-energy asymptotics, thermal explosion, flameless combustion

1. Introduction

The safe storage and transportation of reactant gas mixtures requires conditions that ensure a negligibly small reaction rate, achieved in storage vessels and transport pipes by lowering sufficiently the wall temperature. The seminal investigation of this problem is due to Frank-Kamenetskii (FK) [1], who studied a reacting mixture undergoing an exothermic chemical reaction in a centrally symmetric closed vessel with constant wall temperature. His analysis employed an overall irreversible reaction with an Arrhenius rate having a large activation energy, an appropriate model to represent the strong temperature dependence of

the rate-controlling oxidation reactions in typical fuel-air mixtures [2, 3]. The resulting gas-temperature distribution is seen to depend on the competition of the heat released by the chemical reaction and the heat losses to the wall, characterized by the Damköhler number δ, defined as the ratio of the conduction time across the vessel to the relevant characteristic time (i.e. the homogeneous thermal-explosion time at constant pressure) evaluated at the wall temperature [3]. A slowly reacting flameless mode of combustion is found for values of δ below a critical value, when the heat losses to the wall are able to limit the temperature rise, in such a way that the reaction rate does not change in order of magnitude from its near-wall value. Since the overall heat-release rate is proportional to the volume of reacting gas while the heat-loss rate to the wall is proportional to the wall surface, for a given wall temperature there exists a limiting size, corresponding to a critical value of δ, above which a slow reaction cannot be maintained, and is replaced by a localized temperature runaway that leads to the formation of a flame [4, 5]. More recent analyses of slowly reacting mixtures in closed vessels have addressed additional aspects of the problem, including the effects of pressure increase on the ignition time [6] and of buoyancy-induced motion on explosion limits [7–10].

The results of the FK analysis find direct application in connection with the safety storage of reactant mixtures, defining critical sizes for thermal explosions in chemically reacting systems. A related problem addressed here is that of reactant transportation in pipes, analyzed previously in a simplified configuration [11]. Specifically, we consider below the discharge of a reactant mixture stored in a cold vessel at temperature T_I' through a pipe whose wall temperature is kept at a constant temperature $T_o' > T_I'$ with $T_o' - T_I' \sim T_o'$. The Damköhler number δ introduced by Frank-Kamenetskii for the analysis of thermal explosions in cylindrical vessels emerges as the main governing parameter [11]. Our analysis identifies the existence of an entrance region with negligible chemical reaction, where the gas temperature increases from T_I' towards T_o' by heat conduction from the wall, immediately followed by a region of incipient chemical reaction that governs the transition towards a persistent slowly reacting mode of combustion for $\delta < 2$ or the development of a thermal runaway for $\delta > 2$. Ignition events are analyzed to determine the explosion distance for $\delta > 2$, a computation that requires consideration of the upstream chemically frozen region of temperature accommodation. Specific attention is given to near-critical conditions with delayed ignition events. The development includes also an analytic description of the slowly reacting mode of combustion established downstream the transition region in subcritical configurations with $\delta < 2$.

2. Formulation

Consider a gaseous reactant mixture with initial temperature, density, and reactant mass fraction T_I', ρ_I', and Y_o discharging from a storage vessel along a pipe of radius a whose wall temperature is kept at a fixed value $T_o' > T_I'$. As in Frank-Kamenetskii's work [1], our analysis considers an overall Arrhenius reaction, with the mass of reactant consumed per unit volume per unit time $\dot{m}$ given by

$$\dot{m}/\rho' = k(T')Y_r = B\exp[-E/(RT')]Y_r, \tag{1}$$

where ρ', T', and Y_r represent the density, temperature and reactant mass fraction. The temperature-dependent reaction-rate constant

$$k = B\exp[-E/(RT')] = B\exp[-E/(RT'_o)]\exp[\beta(T'-T'_o)/T'], \tag{2}$$

includes a frequency factor B and an activation energy E, with R denoting the universal gas constant. The characteristic activation temperature E/R is assumed to be large compared with the wall temperature, resulting in a temperature-sensitive rate constant that changes from its wall value $B\exp[-E/(RT'_o)]$ by a factor of order unity when $T'-T'_o \sim RT'^2_o/E = T'_o/\beta \ll T'_o$, where RT'^2_o/E is the so-called FK temperature and $\beta = E/(RT'_o) \gg 1$ is the nondimensional activation energy. A direct consequence of this strong temperature dependence is that, for initially cold mixtures with $T'_o - T'_I \sim T'_o$, the case considered here, the chemical reaction is effectively frozen in the storage vessel.

In this overall-reaction model the heat-release rate of the reaction per unit volume is given by $q\dot{m}$, where q denotes the amount of heat released per unit mass of reactant consumed. Correspondingly, the time t_e needed for the heat-release rate of the chemical reaction—evaluated at T'_o with the initial reactant mass fraction Y_o—to increase the enthalpy by an amount $c_pT'_o/\beta$, proportional to the FK temperature RT'^2_o/E, is given by

$$t_e = \frac{1}{\alpha\beta B\exp[-E/(RT'_o)]}, \tag{3}$$

where $\alpha = (qY_o)/(c_pT'_o)$ is the dimensionless temperature rise, based on T'_o, for constant-pressure adiabatic combustion, with c_p representing the specific heat at constant pressure, taken as constant for simplicity. In relevant combustion applications the parameter α takes values that are of the order of, although typically larger than, unity. The chemical time t_e defined in (3) can be compared with the characteristic heat-conduction time across the pipe

$$t_c = a^2/D_T, \tag{4}$$

where D_T is the thermal diffusivity evaluated at T'_o, to define the FK parameter

$$\delta = t_c/t_e = (a^2/D_T)\alpha\beta B\exp[-E/(RT'_o)], \tag{5}$$

a Damköhler number characterizing the slowly reacting mode of combustion of enclosed reactant mixtures, with the value $\delta = 2$ identifying the explosion limit in cylindrical vessels [1–3].

The discharge is assumed to occur at low Mach numbers, resulting in spatial pressure differences in the pipe that are small compared with the vessel pressure, so that the equation of state can be written in the simplified form $\rho'T' = \rho'_IT'_I$. A convenient characteristic value for the streamwise flow velocity $U = G/(\rho'_o\pi a^2)$ can be defined from the known mass flow rate G by using the density $\rho'_o = \rho'_IT'_I/T'_o$ evaluated at $T' = T'_o$. This velocity defines the Peclet number of the pipe flow $Pe = Ua/D_T$, comparable in magnitude to the associated Reynolds number $Re = Pe/Pr$, with Pr denoting the order-unity Prandtl number of the gaseous mixture. The following analysis pertains to configurations with moderately large values of the Reynolds number $Re \sim Pe$ in the range $10 \lesssim Re \lesssim 2000$, for which the flow in the pipe is stable and slender, with a characteristic streamwise development length $\ell = Pe\,a$

much larger than the pipe radius a. The resulting steady laminar flow can be analyzed in the boundary-layer approximation by integrating

$$\frac{\partial}{\partial x}(\rho u)+\frac{1}{r}\frac{\partial}{\partial r}(r\rho v) = 0 \tag{6}$$

$$\rho u\frac{\partial u}{\partial x}+\rho v\frac{\partial u}{\partial r} = -P_l(x)+\frac{Pr}{r}\frac{\partial}{\partial r}\left(rT^\sigma\frac{\partial u}{\partial r}\right) \tag{7}$$

$$\rho u\frac{\partial T}{\partial x}+\rho v\frac{\partial T}{\partial r} = \frac{1}{r}\frac{\partial}{\partial r}\left(rT^\sigma\frac{\partial T}{\partial r}\right)+\frac{\delta}{\beta}\rho Y\exp[\beta(T-1)/T] \tag{8}$$

$$\rho u\frac{\partial Y}{\partial x}+\rho v\frac{\partial Y}{\partial r} = \frac{1}{Le\,r}\frac{\partial}{\partial r}\left(rT^\sigma\frac{\partial Y}{\partial r}\right)-\frac{\delta}{\alpha\beta}\rho Y\exp[\beta(T-1)/T] \tag{9}$$

for $x>0$ and $0<r<1$ supplemented with the equation of state

$$\rho T=1 \tag{10}$$

and subject to the initial conditions

$$x=0: \quad u-T_{\scriptscriptstyle I}=T-T_{\scriptscriptstyle I}=Y-1=0 \tag{11}$$

at the pipe entrance, and the boundary conditions

$$\frac{\partial u}{\partial r}=v=\frac{\partial T}{\partial r}=\frac{\partial Y}{\partial r}=0 \quad \text{at} \quad r=0 \tag{12}$$

and

$$u=v=T-1=\frac{\partial Y}{\partial r}=0 \quad \text{at} \quad r=1 \tag{13}$$

for $x>0$, as corresponds to axially symmetric flow bounded by a non-permeable constant-temperature wall with non-slip flow.

In the formulation the axial and radial coordinates x' and r' are scaled with $\ell=Pe\,a$ and a according to $x=x'/\ell$ and $r=r'/a$, while their associated velocity components u' and v' are scaled with U and $D_{\scriptscriptstyle T}/a$ to give $u=u'/U$ and $v=v'/(D_{\scriptscriptstyle T}/a)$, respectively. With the scale selected for the axial velocity, its initial uniform value $u'_{\scriptscriptstyle I}=G/(\rho'_{\scriptscriptstyle I}\pi a^2)$ becomes $u'_{\scriptscriptstyle I}/U=\rho'_o/\rho'_{\scriptscriptstyle I}=T_{\scriptscriptstyle I}$ when expressed in dimensionless form, as shown in (11). The reactant mass fraction Y_r is normalized with its initial value Y_o to give $Y=Y_r/Y_o$, and the temperature and density are scaled with T'_o and ρ'_o to give the nondimensional variables $T=T'/T'_o$ and $\rho=\rho'/\rho'_o$. The unknown streamwise pressure gradient $P_l(x)$, to be determined as part of the integration, has been scaled with its characteristic value ρ'_oU^2/ℓ. Its presence in pipe flow ensures mass-flux conservation. Besides the Prandtl number Pr, the Lewis number Le, and the assumed exponent σ for the power-law temperature dependence of the transport coefficients, the problem depends on four nondimensional parameters, namely, the activation energy $\beta=E/(RT'_o)$, the heat-release parameter $\alpha=(qY_o)/(c_pT'_o)$, the Damköhler number δ, and the initial-to-wall temperature ratio $T_{\scriptscriptstyle I}=T'_{\scriptscriptstyle I}/T'_o<1$. The analysis below considers the simplified solution that arises for moderately large values of β with $\alpha\sim 1$, $\delta\sim 1$, and $1-T_{\scriptscriptstyle I}\sim 1$.

3. Sample numerical results

Figure 1 shows results of numerical integrations of (6)–(13) for $\sigma = 0.7$, $Pr = 0.7$, $Le = 1.0$, $\beta = 10$, $\alpha = 5$, and $T_I = 0.5$. A standard Crank-Nicholson method [13] was used to advance the fluid variables in the streamwise direction whereas a collocation technique [14] was used for the radial discretization of the corresponding operators at each axial station. For stability, a modified backward Euler method was used for the initial steps. Typical values of the step size were $\Delta x = 10^{-4}$ for the initial steps and $\Delta x = 10^{-3}$ after 4 or 5 iterations. Computations with both finer and coarser grids were performed to ensure that the results were independent of the grid size.

The plots in Fig. 1 show the evolution along the axis of the temperature $T(x,0)$, reactant mass fraction $Y(x,0)$, and reduced reaction rate $\omega(x,0) = Y \exp[\beta(T-1)/T]$ for two different values of $\delta = (1.0, 5.0)$, along with the corresponding radial profiles of axial velocity at different streamwise locations. The two Damköhler numbers are selected as representative of subcritical and supercritical ignition events. In both cases, the integrations reveal the existence of an initial chemically frozen region, with exponentially small values of $\omega \ll 1$, where the gas temperature increases as a result of the heat transferred from the wall, while the reactant mass fraction does not change significantly. Because of the associated decrease in density, the velocity is seen to increase as its profile evolves from the initial uniform distribution $u = T_I$ towards a parabolic distribution $u = 2(1 - r^2)$.

While the initial evolution is nearly identical for both values of δ, the subsequent downstream evolution is very different. Thus, for $\delta = 1.0$ the reaction rate ω increases to a maximum value of order unity, leading to the establishment of a slowly reacting mode of combustion with $T(x,0)-1 \sim \beta-1$ and small reactant consumption rates $\omega/(\alpha\beta) \sim 1/(\alpha\beta) \ll 1$. By way of contrast, for $\delta = 5$, the reaction rate continues to increase to very large values, leading to a rapid temperature increase at a well defined ignition location $x \simeq 1.32$, where the reactant is rapidly depleted as the temperature reaches its peak value. In the equilibrium region found farther downstream the temperature decreases as a consequence of heat losses to the wall, eventually approaching the wall value $T = 1$ for $x \gg 1$. Following the criterion used in ignition studies in homogeneous systems, the inflection point of the curve $T(x,0)$, marked with a cross in Fig. 1, can be used as a definition of the ignition distance in these computations; other criteria, such as the location of the peak temperature, would give essentially the same results in the limit $\beta \gg 1$.

4. The chemically frozen entrance region

As discussed above, the flow in the tube includes an entrance development region of characteristic length $\ell = Pe\, a$, corresponding to values of x of order unity, where the velocity profile evolves from an initial uniform profile $u = T_I$ to a Poiseuille profile $u = 2(1 - r^2)$ while the temperature evolves from the initial value $T = T_I < 1$ to the wall value $T = 1$. As a consequence of the exponential temperature dependence of the reaction rate discussed earlier, the chemical reaction can be entirely neglected as long as $1 - T \gg \beta^{-1}$, so that the reactant mass fraction remains equal to its initial value $Y = 1$ in this entrance region, as can be seen by integrating the chemically frozen version of (9) with initial condition $Y = 1$ at $x = 0$ and boundary conditions $\partial Y/\partial r = 0$ at $r = 0$ and $r = 1$. The associated distributions

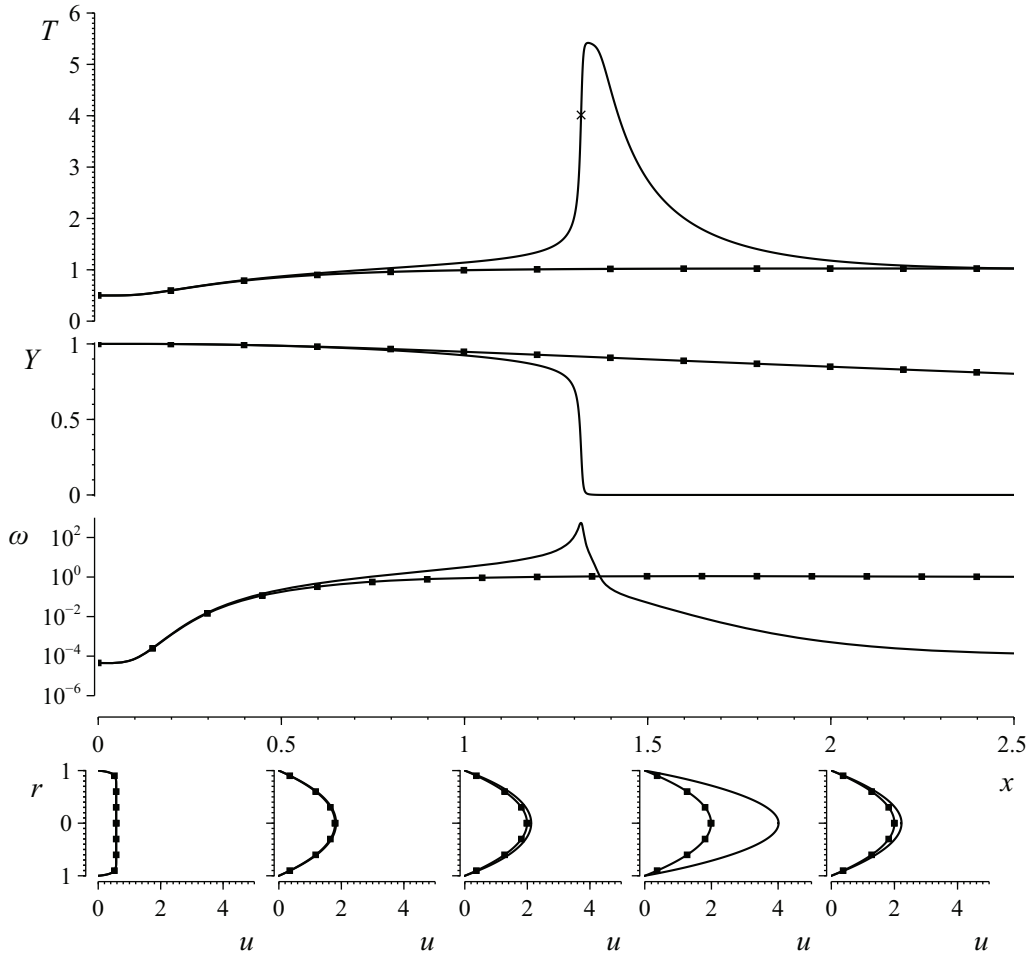

Figure 1: The variation with axial distance of $T(x,0)$, $Y(x,0)$, and $\omega(x,0) = Y\exp[\beta(T-1)/T]$ obtained by numerical integration of (6)–(13) with $\sigma = 0.7$, $Pr = 0.7$, $Le = 1.0$, $\beta = 10$, $\alpha = 5$, and $T_I = 0.5$ for $\delta = 1.0$ (squares) and $\delta = 5.0$ (plain curves); the bottom plots show the axial velocity profiles at five different locations $x = (0, 0.5, 1.0, 1.5, 2.0)$. The cross on the temperature curve for $\delta = 5.0$ indicates the location of the inflection point, used in the numerical integrations to characterize the ignition distance.

of u and T are obtained by integration of (6)–(8) with the initial and boundary conditions given in (11)–(13); the chemical reaction being discarded in (8). The solution depends on the initial temperature T_I and on the transport description through the values of σ and Pr, with the realistic values $\sigma = 0.7$ and $Pr = 0.7$ selected in the integrations reported below, as is appropriate for fuel-air gas mixtures [12].

The resulting chemically frozen, low-Mach-number laminar gas flow has been treated in the past [15–17] to assess effects of variable gas properties on the friction coefficient and heat-transfer rate, including recent efforts to characterize the solution for extreme values of T_I [18]. These previous analyses, which extended to variable density the classical constant-density entry–flow results [19], did not consider specifically the asymptotic behavior of the solution for values of x moderately larger than unity, where the temperature differences from the wall value and of the velocity from the Poiseuille distribution become small. This asymptotic behavior is needed in reacting flows for the analysis of the initiation of the reaction as the temperature increases to near-wall values such that $1 - T \sim \beta^{-1}$. In this region of incipient chemical reaction, located downstream from the entrance region, the heat-transfer rate from the wall changes from positive to negative as a result of the chemical heat release. As seen in Fig. 1, depending on the conditions, the temperature either continues to increase, leading to a thermal runaway at a finite distance downstream, or reaches a maximum value $T-1 \sim \beta^{-1}$ corresponding to a quasisteady balance between the heat released by the chemical reaction and the heat losses to the walls.

The asymptotic temperature distribution for the non-reacting gaseous pipe flow at $x \gg 1$ is given by

$$T - 1 = -C \exp(-\lambda_1^2 x/2) \exp(-\lambda_1 r^2/2) L_{(\lambda_1-2)/4}(\lambda_1 r^2), \tag{14}$$

as can be obtained by using separation of variables in

$$2(1 - r^2)\frac{\partial}{\partial x}(T - 1) = \frac{1}{r}\frac{\partial}{\partial r}\left[r\frac{\partial}{\partial r}(T - 1)\right], \tag{15}$$

derived by linearizing (8) for $T - 1 \ll 1$ with $u \simeq 2(1 - r^2)$ and $v \simeq 0$. Here $L_{(\lambda_1-2)/4}$ is the Laguerre polynomial of order $(\lambda_1 - 2)/4$, with the value of $\lambda_1 = 2.704$ determined as the smallest root of the equation $L_{(\lambda-2)/4}(\lambda) = 0$ associated with the condition $T = 1$ at $r = 1$. The factor C is an unknown positive constant of order unity that must be obtained from the numerical integration of the entrance flow, giving the results shown in Fig. 2. The plot shows the variation with T_I of C and $(2/\lambda_1^2) \ln C$; the latter is to be employed later in evaluating the ignition distance through (24).

5. Slowly reacting flow

The exponential temperature decay (14) is modified as the chemical reaction begins to have a significant effect, which occurs when the temperature drop from the wall value $1 - T$ decreases to values of order β^{-1} across most of the pipe section. The condition $1 - T = \beta^{-1}$ evaluated with use made of the temperature drop along the axis $1-T(x, 0) = C \exp(-\lambda_1^2 x/2)$ given in (14) provides

$$x_d = (2/\lambda_1^2) \ln(C\beta), \tag{16}$$

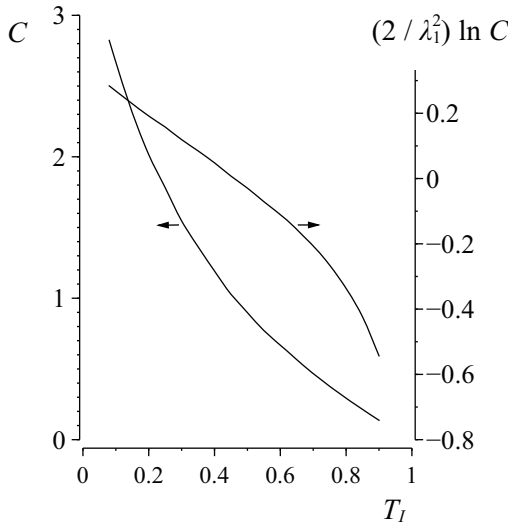

Figure 2: The factor C for the asymptotic temperature distribution (14) found at the end of the chemically frozen entrance region, obtained numerically by fitting (14) to the results of integrations of (6)–(8) with the initial and boundary conditions given in (11)–(13) and with the chemical reaction neglected in (8). The plot also shows the associated value of $(2/\lambda_1^2)\ln C = 0.274\ln C$, which carries in (24) the dependence of the ignition distance on the initial temperature.

as an expression for the downstream location x_d where the reaction becomes important, marking the end of the chemically frozen flow. The following region of incipient chemical reaction, where $T-1 \sim u-2(1-r^2) \sim v \sim \rho-1 \sim \beta^{-1} \ll 1$, can be described in terms of the translated coordinate $\hat{x} = x - x_d$ and the rescaled temperature increment $\theta = \beta(T'-T'_o)/T'_o$, reducing the problem to the integration of

$$2(1-r^2)\frac{\partial\theta}{\partial\hat{x}} = \frac{1}{r}\frac{\partial}{\partial r}\left(r\frac{\partial\theta}{\partial r}\right) + Y\delta \mathrm{e}^{\theta} \tag{17}$$

$$2(1-r^2)\frac{\partial Y}{\partial\hat{x}} = \frac{1}{Le\, r}\frac{\partial}{\partial r}\left(r\frac{\partial Y}{\partial r}\right) - \frac{1}{\alpha\beta}Y\delta \mathrm{e}^{\theta} \tag{18}$$

with initial conditions

$$\theta + \exp(-\lambda_1^2\hat{x}/2)\exp(-\lambda_1 r^2/2)L_{(\lambda_1-2)/4}(\lambda_1 r^2) = Y - 1 = 0 \quad \text{as} \quad \hat{x} \to -\infty \tag{19}$$

and boundary conditions

$$\frac{\partial\theta}{\partial r} = \frac{\partial Y}{\partial r} = 0 \quad \text{at} \quad r = 0 \qquad \text{and} \qquad \theta = \frac{\partial Y}{\partial r} = 0 \quad \text{at} \quad r = 1. \tag{20}$$

The initial conditions for integration of (17) and (18), given in (19), are obtained by matching with the solution found in the entrance region at intermediate distances $1 \ll x \ll x_d$, corresponding to large negative values of the translated coordinate $\hat{x} = x - x_d$, represented by the limit $\hat{x} \to -\infty$ in (19). In particular, the initial temperature distribution is obtained by writing the temperature profile (14) in terms of $\hat{x} = x - x_d$ with use made of (16). The Frank-Kamenetskii linearization $\exp[\beta(T-1)/T] = \exp[\theta/(1+\theta/\beta)] \simeq \mathrm{e}^{\theta}$ has been employed in writing the reaction rate in (17) and (18), as it is appropriate in the limit $\beta \gg 1$ with $\theta \sim 1$.

6. The first reaction stage

The analysis of the chemical reaction at distances $\hat{x} = x - x_d \sim 1$ determines whether the solution undergoes a thermal runaway, as occurs for supercritical cases with $\delta > 2$, or whether the flow evolves into a quasisteady slow mode of combustion that persists farther downstream, as occurs for $\delta \leq 2$. In this transition region $x \sim 1$ with $\theta \sim 1$ the change in reactant mass fraction is small, of order $1 - Y \sim (\alpha\beta)^{-1} \ll 1$, as follows from (18), so that the problem reduces to the integration of

$$2(1 - r^2)\frac{\partial \theta}{\partial \hat{x}} = \frac{1}{r}\frac{\partial}{\partial r}\left(r\frac{\partial \theta}{\partial r}\right) + \delta \mathrm{e}^{\theta} \tag{21}$$

subject to the initial and boundary conditions given above in (19) and (20). Selected results of computations are shown in Fig. 3. In the integrations, a low-storage standard RKW3 method [20] was used for advancing in $\hat{x}$ with a variable step size with minimum value $\Delta\hat{x} = 10^{-3}$. The pseudospectral technique [14] used previously in integrating (6)–(13) was employed for the radial discretization of (21). The integration was initiated with the temperature profile given in (19) evaluated at a selected negative value of $\hat{x}$ and the results were found to be independent of the selection for values of the initial location smaller than -1.

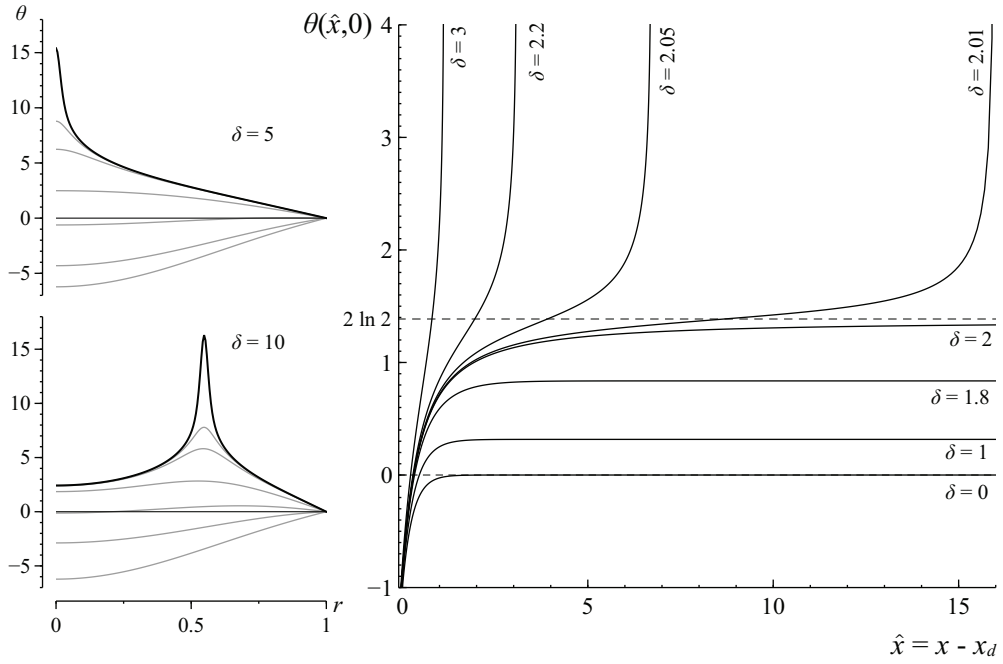

Figure 3: The temperature evolution obtained by integration of (21) with the initial and boundary conditions given in (19) and (20) for different values of δ, including the evolution with distance of the temperature along the axis $\theta(\hat{x}, 0)$ for subcritical and supercritical cases along with selected temperature profiles for $\delta = 5$ $[\hat{x} = (0, 0.999, 4.999, 9.299, 9.678, 9.686, 9.687)]$ and $\delta = 10$ $[\hat{x} = (0, 2.010, 4.826, 5.933, 6.028, 6.032, 6.033)]$.

For subcritical cases with $\delta \leq 2$ the temperature evolves towards the steady distribution

$$\theta_{\mathrm{FK}} = 2\ln\left\{\frac{2/(1 + \sqrt{1 - \delta/2})}{1 + (\delta/2)[r/(1 + \sqrt{1 - \delta/2})]^2}\right\} \tag{22}$$

corresponding to the cylindrical FK problem

$$\frac{1}{r}\frac{\mathrm{d}}{\mathrm{d}r}\left(r\frac{\mathrm{d}\theta_{\mathrm{FK}}}{\mathrm{d}r}\right) = -\delta\, e^{\theta_{\mathrm{FK}}}, \quad \frac{\mathrm{d}\theta_{\mathrm{FK}}}{\mathrm{d}r}(0) = \theta_{\mathrm{FK}}(1) = 0. \tag{23}$$

The associated temperature along the axis $\theta(\hat{x},0)$ is seen to approach $\theta(\hat{x},0) = 2\ln[2/(1+\sqrt{1-\delta/2})]$ for $x \gg 1$, with the limiting value $\theta(\hat{x},0) = 2\ln 2$ reached for the critical case $\delta = 2$.

On the other hand, for $\delta > 2$ the transition stage ends with a thermal runaway at a finite downstream location $\hat{x}_t = x_t - x_d \sim 1$. An interesting finding of the numerical integrations of the ignition problem (21), illustrated in the transient histories on the left-hand side of Fig. 3, is that the thermal runaway occurs at the axis for values of δ in the range $2 < \delta \lesssim 6.68$, whereas for $\delta \gtrsim 6.68$ the thermal runaway occurs in an increasingly thinner annular reacting layer at an intermediate radius, not far from the wall, while the gas in the center is still cold. A similar behavior was identified in [6] in connection with the transient ignition history in spherical containers.

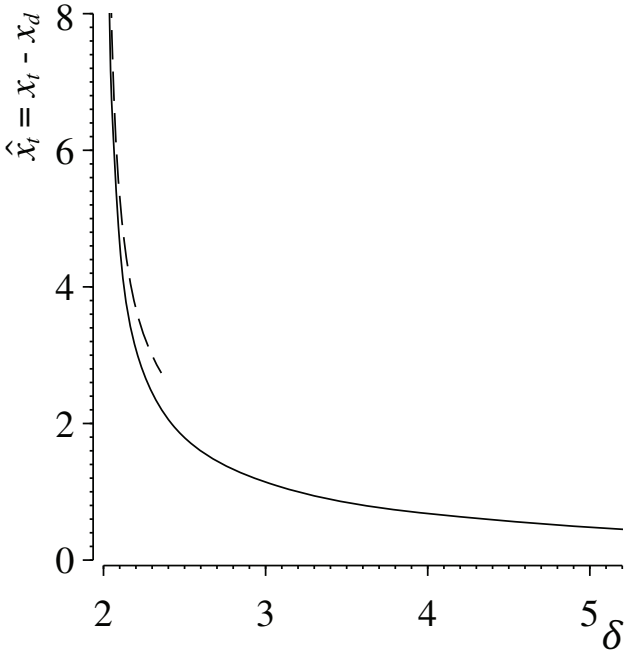

Figure 4: The variation with $\delta > 2$ of the thermal-runaway distance $\hat{x}_t = x_t - x_d$, with the dashed curve representing the near-critical asymptotic result (32).

The resulting thermal-runaway location $\hat{x}_t$, a decreasing function of δ, is shown in Fig. 4. The ignition distance computed here differs by a factor of order unity from that computed earlier in [11], where integrations of (21) were started with an initially uniform gas temperature, equal to the wall value. The present analysis, accounting for the presence of the reaction-free entry region, provides a prediction for the distance from the entrance of the pipe x_t' at which ignition occurs, given in nondimensional form $x_t = x_t'/[G/(\pi\rho_o' D_T)]$ by

$$x_t = x_d(T_I, \beta) + \hat{x}_t(\delta) = (2/\lambda_1^2)\ln C + (2/\lambda_1^2)\ln\beta + \hat{x}_t, \tag{24}$$

written with use made of (16). As can be seen, the value of x_t results from the addition of three separate terms that carry the influence of T_I, β, and δ, respectively. The first and third terms are given in Figs. 2 and 4, respectively, whereas the second term can be readily evaluated using $2/\lambda_1^2 \simeq 0.274$.

7. Ignition for near-critical conditions $\delta - 2 \ll 1$

For $0 < \delta - 2 \ll 1$ the thermal runaway occurs at very large distances $\hat{x}_t \gg 1$. As can be inferred from the results for $\delta = 2.01$ shown on the right-hand side of Fig. 3, for these near-critical conditions the ignition history includes a relatively short initial period $\hat{x} \sim 1$, where the temperature increases to approach the critical FK profile $\theta_{\rm FK} = 2\ln[2/(1+r^2)]$ corresponding to $\delta = 2$, followed by a long quasi-steady evolution for $\hat{x} \sim (\delta-2)^{-1/2} \gg 1$ with $\theta - 2\ln[2/(1+r^2)] \sim (\delta-2)^{1/2} \ll 1$ which ends with a thermal runaway. This second stage can be investigated in terms of the asymptotically small parameter $\varepsilon = \delta/2 - 1$ to determine the resulting value of $\hat{x}_t \sim \varepsilon^{-1/2} \gg 1$.

The development begins by writing (21) in terms of the rescaled coordinate $\xi = \varepsilon^{1/2}\hat{x}$ and the off-equilibrium temperature departure $\theta - 2\ln[2/(1+r^2)] = \varepsilon^{1/2}\Theta(\xi, r)$ to give

$$2(1-r^2)\varepsilon\frac{\partial\Theta}{\partial\xi} = \frac{\varepsilon^{1/2}}{r}\frac{\partial}{\partial r}\left(r\frac{\partial\Theta}{\partial r}\right) + \frac{8}{(1+r^2)^2}\left[(1+\varepsilon)\mathrm{e}^{\varepsilon^{1/2}\Theta} - 1\right]. \tag{25}$$

Introducing the expansion $\Theta = \Theta_1 + \varepsilon^{1/2}\Theta_2 + \cdots$ and collecting terms of order $\varepsilon^{1/2}$ leads to

$$\frac{1}{r}\frac{\partial}{\partial r}\left(r\frac{\partial\Theta_1}{\partial r}\right) + \frac{8\Theta_1}{(1+r^2)^2} = 0; \qquad \frac{\partial\Theta_1}{\partial r} = 0 \text{ at } r = 0 \quad \text{and} \quad \Theta_1 = 0 \text{ at } r = 1, \tag{26}$$

which can be integrated to give

$$\Theta_1 = F(\xi)\frac{1-r^2}{1+r^2}. \tag{27}$$

The unknown function $F(\xi)$, carrying the streamwise dependence of the off-equilibrium temperature departure, can be obtained from the problem arising at order ε

$$\frac{1}{r}\frac{\partial}{\partial r}\left(r\frac{\partial\Theta_2}{\partial r}\right) + \frac{8\Theta_2}{(1+r^2)^2} = Q(\xi, r); \qquad \frac{\partial\Theta_2}{\partial r} = 0 \text{ at } r = 0 \quad \text{and} \quad \Theta_2 = 0 \text{ at } r = 1, \tag{28}$$

where

$$Q = 2\frac{(1-r^2)^2}{1+r^2}\frac{\mathrm{d}F}{\mathrm{d}\xi} - \frac{8}{(1+r^2)^2}\left[1 + \frac{1}{2}\left(\frac{1-r^2}{1+r^2}\right)^2 F^2\right]. \tag{29}$$

Existence of solutions to the inhomogeneous problem (28) requires that $\int_0^1 Q(1-r^2)r/(1+r^2)\mathrm{d}r = 0$, providing the ordinary differential problem

$$\frac{1}{2}\frac{\mathrm{d}F}{\mathrm{d}\xi} = \frac{1+(F/2)^2}{17 - 12\ln 4}; \qquad F(0) = -\infty, \tag{30}$$

where the initial condition $F(0) = -\infty$ follows from matching with the upstream region $\hat{x} \sim 1$ of rapid temperature increase. The solution

$$F = 2\tan\left(\frac{\xi}{17 - 12\ln 4} - \frac{\pi}{2}\right) \tag{31}$$

diverges as $\xi \to \xi_t = (17 - 12\ln 4)\pi$, as corresponds to a thermal-runaway distance

$$\hat{x}_t = \varepsilon^{-1/2}\xi_t = \frac{(17 - 12\ln 4)\sqrt{2}\pi}{(\delta - 2)^{1/2}} \simeq 1.62(\delta - 2)^{-1/2}. \tag{32}$$

This asymptotic prediction is shown as a dashed curve in Fig. 4.

As noted earlier in connection with the homogeneous ignition problem [21], reactant consumption, not accounted for in the ignition equation (21), would necessarily become significant in configurations with sufficiently small values of $\delta - 2$, thereby modifying the result (32) as well as the thermal explosion limiting condition $\delta = 2$, with associated departures $\delta - 2$ that can be anticipated to be of order $1/(\alpha\beta) \ll 1$ [6].

8. Downstream flameless combustion for $\delta \leq 2$

For subcritical values of the Damköhler number $\delta \leq 2$ the temperature in the pipe evolves towards the quasi-steady distribution (22) for moderately large values of $\hat{x}$. Most of the reactant consumption, negligibly small in the entrance and transition regions, occurs downstream, at distances of order $\alpha\beta\ell$, such that the rescaled coordinate $X = (x - x_d)/(\beta\alpha)$ is of order unity, when (17) and (18) become

$$\frac{2}{\alpha\beta}(1 - r^2)\frac{\partial\theta}{\partial X} = \frac{1}{r}\frac{\partial}{\partial r}\left(r\frac{\partial\theta}{\partial r}\right) + Y\delta \mathrm{e}^{\theta}, \tag{33}$$

$$2(1 - r^2)\frac{\partial Y}{\partial X} = \frac{\alpha\beta}{Le\, r}\frac{\partial}{\partial r}\left(r\frac{\partial Y}{\partial r}\right) - Y\delta \mathrm{e}^{\theta}, \tag{34}$$

to be solved with the boundary conditions given earlier. Equation (34) indicates that during this second stage transverse diffusion of the reactant is so fast that its mass fraction remains spatially uniform across the pipe at leading order, so that $Y \simeq \bar{Y}(X)$ with errors of order $1/(\alpha\beta)$, while the temperature evolves in a quasi-steady manner as dictated by

$$\frac{1}{r}\frac{\partial}{\partial r}\left(r\frac{\partial\theta}{\partial r}\right) + \bar{Y}\delta \mathrm{e}^{\theta} = 0, \tag{35}$$

the limiting form of (33) for $\beta\alpha \gg 1$.

As can be inferred from (23), the solution to (35) subject to $\partial\theta/\partial r = 0$ at $r = 0$ and $\theta = 0$ at $r = 1$ is just given by

$$\theta = 2\ln\left\{\frac{2/(1 + \sqrt{1 - \delta\,\bar{Y}/2})}{1 + (\delta\,\bar{Y}/2)[r/(1 + \sqrt{1 - \delta\,\bar{Y}/2})]^2}\right\} \tag{36}$$

obtained by writing the FK temperature distribution (22) with δ replaced by the instantaneous Damköhler number $\delta\,\bar{Y}$. The evolution of $\bar{Y}(X)$ is given by

$$\frac{\mathrm{d}\bar{Y}}{\mathrm{d}X} = -2\int_0^1 \delta\,\bar{Y}\mathrm{e}^{\theta} r\,\mathrm{d}r, \qquad \bar{Y}(0) = 1, \tag{37}$$

obtained by integrating (34) multiplied by r, with use made of the non-permeability condition $\partial Y/\partial r = 0$ at $r = 1$. Since the energy balance is quasi-steady, the surface integral in (37),

representing the overall rate of reactant consumption across the pipe, is proportional to the rate of heat transfer to the wall, as can be seen by using (35) to write (37) in the alternative form

$$\frac{1}{2}\frac{\mathrm{d}\bar{Y}}{\mathrm{d}X} = \int_0^1 \frac{\partial}{\partial r}\left(r\frac{\partial\theta}{\partial r}\right)\mathrm{d}r = \left(\frac{\partial\theta}{\partial r}\right)_{r=1}, \qquad \bar{Y}(0) = 1, \tag{38}$$

involving the reduced heat-loss rate to the wall

$$-\left(\frac{\partial\theta}{\partial r}\right)_{r=1} = \frac{\delta\bar{Y}}{1+\sqrt{1-\delta\,\bar{Y}/2}} \tag{39}$$

evaluated with use made of (36). Substituting (39) into (38) and integrating the resulting separable equation finally yields

$$\delta X = \left(1-\frac{\delta}{2}\right)^{1/2} - \left(1-\frac{\delta\bar{Y}}{2}\right)^{1/2} - \ln\left[\frac{1-\left(1-\delta\bar{Y}/2\right)^{1/2}}{1-(1-\delta/2)^{1/2}}\right] \tag{40}$$

as an implicit representation for the reactant mass fraction as a function of the rescaled streamwise distance $X = (x - x_d)/(\alpha\beta)$. The above expression applies for subcritical cases with $\delta \leq 2$.

9. Accuracy of the analytical predictions

The leading-order asymptotic analyses given above provide predictions of ignition distances for $\delta > 2$ and of slow flameless reactant consumption for $\delta < 2$ that apply strictly in the limit $\beta \gg 1$. It is therefore worthwhile to test the accuracy of these predictions for large but finite values of β, by comparing the analytical results with numerical integrations of the starting equations (6)–(13).

We begin by comparing in Fig. 5 the ignition distance predicted by the expression (24) with that obtained numerically, with the inflection-point criterion employed to give a precise definition of x_t in the computations. A first set of computations, shown in the upper plot, consider increasing values of β for a fixed value of $\delta = 5$. The accuracy of the asymptotic results is seen to improve for increasing β, yielding corresponding relative errors that decrease in proportion to β^{-1}, as expected from the ordering of the corrections in the asymptotic description.

A second set of computations, for a fixed value of $\beta = 32$, considers ignition histories for different values of δ. The results are shown in the bottom plot of Fig. 5. As can be seen, the accuracy of the prediction degrades as the ignition distance increases for smaller values of δ. The observed departures are attributable to the effect of reactant consumption, neglected in our leading-order analysis, which becomes more noticeable for longer residence times, slowing down the reaction rate and leading to values of x_t that are larger than those predicted by (24). Incorporation of these reactant-consumption effects in the asymptotic analysis would require consideration of corrections of order β^{-1}, following the methodology developed earlier for the homogeneous problem [21].

According to the asymptotic results, in the flameless mode of combustion established in the pipe for $\delta \leq 2$ the resulting reactant mass fraction, uniform across the pipe, decreases

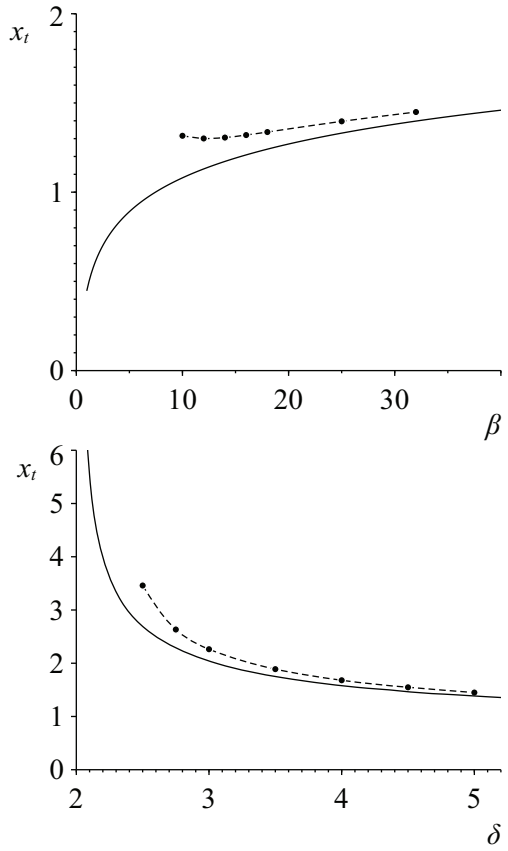

Figure 5: The ignition distance for $T_I = 0.5$ obtained with the inflection-point criterion from numerical integrations of (6)–(13) for $\sigma = 0.7$, $Pr = 0.7$, $Le = 1.0$, and $\alpha = 5$ (circles) and evaluated with the asymptotic prediction (24) (solid lines). The upper plot shows the variation of x_t with β for $\delta = 5.0$ while the lower plot shows the variation of x_t with δ for $\beta = 32$.

slowly with $X = (x - x_d)/(\beta\alpha)$ as dictated by (40), whereas the temperature increment from the wall value $T - 1 \sim \beta^{-1}$ follows the quasi-steady distribution (36), with a corresponding value at the axis given by

$$T(x,0) = 1 + 2\beta^{-1} \ln \left[2 \Big/ \left(1 + \sqrt{1 - \delta\, \bar{Y}/2} \right) \right]. \tag{41}$$

These predictions are shown in Fig. 6 along with numerical results for $\beta = 10$ and $\delta = (0.5, 1.0)$, the latter shown as solid curves. As can be seen, the dashed curves representing the analytical results fall on top of the solid curves from $x \sim 1$ all the way to the reactant depletion region, located at $x \simeq 50$ for $\delta = 1$ and at $x \simeq 100$ for $\delta = 0.5$. The degree of agreement achieved is truly remarkable, indicating that the leading-order results developed here are sufficiently accurate to describe reactant consumption in flameless combustion in pipes for large but finite values of β.

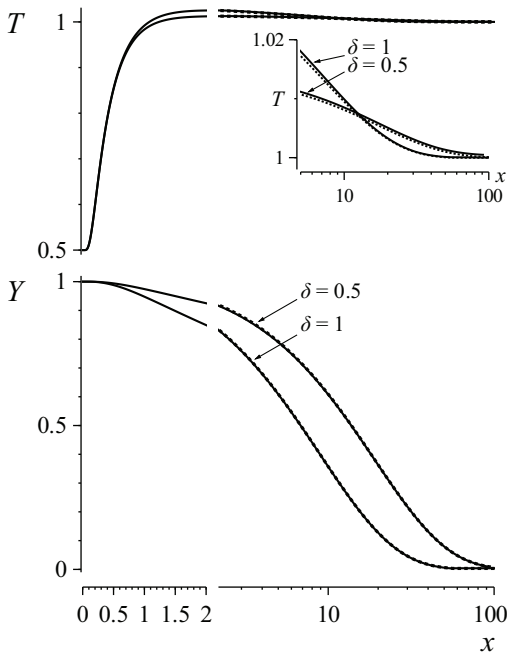

Figure 6: The solid curves represent the evolution of the temperature and reactant mass fraction along the axis obtained by numerical integration of (6)–(13) with $\sigma = 0.7$, $Pr = 0.7$, $Le = 1.0$, $\beta = 10$, $\alpha = 5$, and $T_I = 0.5$ for two different subcritical values of δ, whereas the dashed curves are the predicted value of $\bar{Y}$, obtained by evaluating (40) with use made of $X = (x - x_d)/(\beta\alpha)$ and (16), and of the accompanying temperature along the axis, determined from (41).

10. Concluding remarks

The flow of an initially cold reactant mixture in a hot cylindrical pipe at moderately large values of the Reynolds number has been analyzed in the limit of large activation energies. The flow includes an entrance region where the gas temperature adapts to the wall value, followed by a shorter region of incipient reaction where the flow evolves to give either a rapid thermal runaway leading to the generation of a flame or a quasi-steady flameless mode of combustion that persists downstream along the pipe. Appropriate rescaled problems have been formulated and analyzed in the different regions, leading to predictions for the ignition distance in supercritical cases and for the slow downstream reactant consumption encountered in subcritical cases. While the present analysis pertains only to the classical one-step Arrhenius heat-release description underlying the FK theory, future studies of flameless combustion in pipes incorporating realistic chemistry are clearly worth pursuing, using for instance reduced chemical-kinetic mechanisms, an approach that has been found to be useful in developing analytical predictions of explosion limits for hydrogen-oxygen systems [22, 23]. Also, extensions of the analysis to address more general boundary conditions for the temperature at the wall could be attempted, for instance by consideration of a Newtonian heat–exchange law, as done previously for thermal explosions in closed vessels [3]. Effects of buoyancy-induced motion are also worth exploring, including modifications to the critical value $\delta = 2$ arising from enhanced heat-transfer rates, which could be described for small Rayleigh numbers using a perturbation analysis similar to that performed recently in [10].

Acknowledgements

This work was supported by the Spanish MCINN through project # CSD2010-00010. Fruitful discussions with Amable Liñán and Forman Williams are gratefully acknowledged.

References

[1] D.A. Frank-Kamenetskii, The temperature distribution in a reaction vessel and the time-independent theory of thermal explosions, Zh. Fiz. Khim 13 (1939) 738–755.

[2] D.A. Frank-Kamenetskii, Diffusion and heat transfer in chemical kinetics, Second ed., Plenum Press, New York, NY, 1969.

[3] Ya. B. Zel'dovich, G. I. Barenblatt, V. B. Librovich, and G. M. Makhviladze, The Mathematical Theory of Combustion and Explosions, Consultants Bureau, New York., 1985.

[4] J.W. Dold, Analysis of the early stage of thermal runaway, Q. J. Mech. Appl. Math. 38 (1985) 361–387.

[5] J.W. Dold, Analysis of thermal runaway in the ignition process, SIAM J. Appl. Math. 49 (1989) 459–480.

[6] A. Liñán, D. Moreno-Boza, I. Iglesias, A.L. Sánchez, F. A. Williams, The slowly reacting mode of combustion of gaseous mixtures in spherical vessels. Part 1: transient analysis and explosion limits, Combust. Theor. Model. 20 (2016) 1010–1028.

[7] L. Kagan, H. Berestycki, G. Joulin, G. Sivashinsky, The effect of stirring on the limits of thermal explosion, Combust. Theory Model. 1 (1997) 97–111.

[8] T.-Y. Liu, A.N. Campbell, S.S.S. Cardoso, A.N. Hayhurst, Effects of natural convection on thermal explosion in a closed vessel, Phys. Chem. Chem. Phys. 10 (2008) 5521–5530.

[9] T.-Y. Liu, A.N. Campbell, A.N. Hayhurst, S.S.S. Cardoso, On the occurrence of thermal explosion in a reacting gas: The effects of natural convection and consumption of reactant, Combust. Flame 157 (2010) 230–239.

[10] A.L. Sánchez, I. Iglesias, D. Moreno-Boza, A. Liñán, F. A. Williams, The slowly reacting mode of combustion of gaseous mixtures in spherical vessels. Part 2: buoyancy-induced motion and its effect on the explosion limits, Combust. Theor. Model. 20 (2016) 1029–1045.

[11] G.I. Barenblatt, A.J. Chorin, and A. Kast, The influence of the flow of the reacting gas on the conditions for a thermal explosion, Proc. Natl. Acad. Sci. USA 94 (1997) 12762–12764.

[12] D.E. Rosner, Transport processes in chemically reacting flow systems, Dover Publications, Inc., Mineola, New York, 2000.

[13] D.A. Anderson, J.C. Tannehill, R.H. Pletcher, Computational fluid mechanics and heat transfer, Second ed., CRC Press, Boca Raton, Florida, 1984, p. 499.

[14] T.A. Driscoll, N. Hale, L.N. Trefethen, editors, Chebfun Guide, Pafnuty Publications, Oxford, 2014.

[15] W. M. Kays, W. B. Nicoll, Laminar flow heat transfer to a gas with large temperature differences, ASME J. Heat Transfer 85 (1963) 329–338.

[16] E. Davenport, G. Leppert, The effect of transverse temperature gradients on the heat transfer and friction for laminar flow of gases, ASME J. Heat Transfer 87 (1965) 191–196.

[17] M. Worsoe-Schmidt, G. Leppert, Heat transfer and friction for laminar flow of a gas in a circular tube at a high heating rate, Int. J. Heat Mass Transfer 8 (1965) 1291–1301.

[18] F. J. Higuera, Laminar flow of a gas in a tube with large temperature differences, Phys. Fluids 23 (2011) 123602.

[19] L.L. Crabtree, D. Küchemann, L. Sowerby, Three-dimensional boundary layers, in: L. Rosenhead (Ed.), Laminar Boundary Layers, Dover Publications Inc., New York, 1988, pp. 409-491.

[20] P.R. Spalart, R.D. Moser, M.M. Rogers. Spectral methods for the Navier-Stokes equations with one infinite and two periodic directions, J. Comp. Phys. 96 (1991) 297–324.

[21] D. R. Kassoy, A. Liñán, The influence of reactant consumption on the critical conditions for homogeneous thermal explosions, Q. J. Mech. Appl. Math. 31 (1978) 99–112.

[22] A.L. Sánchez, E. Fernández-Tarrazo, F.A. Williams, The chemistry involved in the third explosion limit of H_2-O_2 mixtures, Combust. Flame 161 (2014) 111–117.

[23] A.L. Sánchez, F.A. Williams, Recent advances in understanding of flammability characteristics of hydrogen, Prog. Energy Combust. Sci. 41 (2014) 1–55.